

Access to Monomeric Hydridoplumbate(II) Anions with Remarkable Thermostability

Shuo Wang

National Yang Ming Chiao Tung University

Han-Jung Li

Industrial Technology Research Institute

Wan-Ching Lee

National Chung Hsing University

Shuo-Ling Huang

National Taiwan University

Wen-Chun Wu

Rezwave Technology Inc.

Fong-Ku Shi

Rezwave Technology Inc.

Ting-Shen Kuo

National Normal Taiwan University

I-Chung Lu

National Chung Hsing University <https://orcid.org/0000-0002-3125-6397>

Hsueh-Ju Liu (✉ hsuehjuli@nycu.edu.tw)

National Yang Ming Chiao Tung University <https://orcid.org/0000-0002-8437-1479>

Article

Keywords: Monomeric Hydridoplumbate(II), thermostability

Posted Date: August 26th, 2021

DOI: <https://doi.org/10.21203/rs.3.rs-812025/v1>

License:   This work is licensed under a Creative Commons Attribution 4.0 International License.

[Read Full License](#)

Abstract

We report on the remarkable stability of synthesized monomeric hydridoplumbates $M^+[LPb(II)H]^-$ ($M[1-H]$) where $L = 2,6$ -bis(3,5-diphenylpyrrolyl)pyridine and $M = (18\text{-crown-6})\text{potassium}$ or $([2.2.2]\text{-cryptand})\text{potassium}$. The half-life of $[K18c6][1-H]$ is approximately 2 days in tetrahydrofuran at ambient temperature. The presence of a Pb–H bond in the hydridoplumbates was unambiguously identified by performing 1H , 2H (with a lead(II) deuteride analogue), $^{207}Pb\{^1H\}$, proton-coupled ^{207}Pb , and $^1H\text{-}^{207}Pb$ 2D nuclear magnetic resonance spectroscopy. The experimental observations and theoretical calculations indicated the presence of dihydrogen bonding as a secondary coordination sphere interaction between the protons of the ligand backbone and the hydride ligand that helps stabilize Pb–H bonding. The Pb–H bond readily adds to the C = O bond of benzaldehyde to form a benzyloxy compound. The regeneration of Pb(II)–H moieties was observed by treating pinacolborane with lead(II) benzyloxy compounds, which indicated that lead(II) hydrides can be used as catalysts for hydroelementation reactions involving unsaturated molecules.

Introduction

Power et al. were the first researchers to report on the low-valent Sn(II) hydride species $^1Ar^{iPr6}Sn(\mu\text{-}H)_2SnAr^{iPr6}$ ($Ar^{iPr6} = [C_6H_3\text{-}2,6\text{-}(C_6H_2\text{-}2,4,6\text{-}iPr_3)_2]^-$); since then, considerable progress has been made by several research groups in areas such as the isolation and reactivity of divalent group-14 hydrides^{2,3}. The heavier group-14 elements' orbitals that participate in E(II)–H bonds (E = Si, Ge, Sn, and Pb) are almost p -based due to the increased energy gap between s - and p -orbitals upon descending the group, resulting in weak tendency to hybridize⁴. Therefore, the E(II)–H bonds in hydridotetrylenes are weaker and more reactive than E(IV)–H bonds that comprise sp^3 orbitals of tetravalent congeners. This property is reflected in the notable reactivity of low-valent hydridotetrylenes (for Si, Ge, and Sn), particularly during the catalyst-free hydroelementation of unreactive substrates, a process that has demonstrated good potential for organic synthesis³. Nevertheless, few studies have explored the development of Pb(II) hydride chemistry, likely to the extremely fragile Pb(II)–H bonds. Early studies of Pb–H chemistry mostly focused on the hydroplumbylation of alkylated Pb(IV) compounds such as R_3PbH (R = Me, Et, nBu , etc.) with unsaturated molecules^{5,6}. Transient lead hydride species can also be generated through the reaction of laser-ablated Pb atoms with, for example, H_2 ⁷, CH_4 ⁸, and SiH_4 at low temperature⁹, and can be observed using infrared spectroscopy. Per their recent theoretical results, Toro-Labbé et al. predicted that a β -diketiminato ligand–supported lead(II) hydride complex is superior to its Ge(II) and Sn(II) analogues as a catalyst for CO_2 activation¹⁰.

A seminal report by Power et al. describes the synthesis of the first diplumbyne $[Ar^{iPr6}Pb\text{-}PbAr^{iPr6}]$, which was obtained by treating $Ar^{iPr6}PbBr$ with $LiAlH_4$ and, thus, implicating the elusive formation of a Pb(II)–H intermediate during the reaction. The formation of the aforementioned intermediate was also speculated in hydroboration studies of phosphine-stabilized plumbylene compound $[Ar^{iPr6}PbCH(Ph)PPh_2]$ in which

diplumbyne $[\text{Ar}^{\text{iPr6}}\text{Pb}-\text{PbAr}^{\text{iPr6}}]$ was isolated after a reaction by Wesemann and co-workers¹¹. This hypothesis was only recently verified by the Wesemann and Power groups^{12,13}. These two groups independently isolated the dimeric Pb(II) hydride compound $[\text{ArPb}(\mu\text{-H})]_2$ ($\text{Ar} = \text{Ar}^{\text{iPr6}}$, $[\text{C}_6\text{H}_3\text{-2,6-(C}_6\text{H}_3\text{-2,6-}^{\text{iPr2}}\text{)}_2]^-$ (Ar^{iPr4}), and $[\text{C}_6\text{H}_3\text{-2,6-(C}_6\text{H}_2\text{-2,4,6-Me}_3\text{)}_2]^-$ (Ar^{Me6}); Fig. 1) by treating bulky terphenyl-supporting lead precursors with the appropriate hydride reagents at low temperatures, and they confirmed that the diplumbynes (for Ar^{iPr6} and Ar^{iPr4}) were the decomposition products of Pb(II) hydride compounds. Notably, these dimeric compounds, which are supported by bulky terphenyl ligands, are the only known hydrides of Pb(II). The dearth of stable and monomeric Pb(II) hydride species has motivated researchers to continue exploring new types of synthons that can support this type of reactive fragment.

In our previous paper, we reported the synthesis of a low-valent tri-tin complex $(\text{dpp}^{\text{Ph}}\text{Sn})_3\text{Cl}$ through the reduction of $\text{dpp}^{\text{Ph}}\text{SnCl}$ with $\text{LiB}^{\text{s}}\text{Bu}_3\text{H}$ ($\text{dpp}^{\text{Ph}} = 2,5\text{-di(o-pyridyl)-3,4-diphenylpyrrolate}$), which contains two Sn–Sn linkages that are perpendicular to the dpp^{Ph} ligand planes¹⁴. This indicates that the occupation of the p_x and p_y orbitals of Sn centers by planar pincer dpp^{Ph} ligands allows for further development along the axial (or z) directions (by using the p_z orbitals of Sn). Compared with the monoanionic dpp^{Ph} ligand, which forms Sn(II) complexes with an X-type ligand in the axial position, the dianionic [2,6-bis(3,5-diphenylpyrrolyl)pyridine] ligand¹⁵ (denoted **L** hereafter) was proposed to support an E(II) center with an empty orbital and a lone pair of electrons and, thus, exhibit a new type of reactivity (E = heavier group-14 elements; Fig. 2). In this study, we demonstrated that the neutral and Lewis acidic “**LPb**” fragment is a favorable platform for stabilizing Pb(II)–H bonding to form monomeric hydridoplumbates $\text{M}^+[\text{LPbH}]^-$ (**M[1-H]**) with an uncommon level of stability, where **L** = 2,6-bis(3,5-diphenylpyrrolyl)pyridine and **M** = (18-crown-6)K, or ([2.2.2]-crypt)K. Reactivity studies of $\text{M}^+[\text{LPbH}]^-$ highlighted that these species can be used as catalysts for carbonyl hydroboration reactions.

Results

Synthesis of **M[1-H]** complexes

Treatment of H_2L with 1 equiv of $\text{Pb}(\text{HMDS})_2$ ($\text{HMDS} = \text{N}(\text{SiMe}_3)_2$) afforded an insoluble orange-red solid in 95% yield in weakly-coordinating solvents, such as benzene and toluene, which is likely polymeric or oligomeric $\{\text{LPb}\}_n$. Upon “dissolution” in tetrahydrofuran (THF), this compound reacted with the solvent to form $\text{LPb}(\text{THF})_2$ (**1-THF**₂; “**1**” represents the “**LPb**” fragment). After recrystallization, **1-THF**₂ was obtained in 85% yield as an orange-red crystalline solid, and its identity was verified using elemental analysis, multinuclear nuclear-magnetic-resonance (NMR) spectroscopy, and X-ray crystallography. The ²⁰⁷Pb NMR spectroscopy of five-coordinate **1-THF**₂ revealed a single resonance at 422.8 ppm, which was shifted upfield compared with the resonance of three-coordinate, β-diketiminato-supported chloro-, amido-, and alkyl-plumbylenes (approximately 3000–1400 ppm)¹⁶⁻¹⁸. The coordination of THF molecules on the axial positions of “**LPb**” reveals its Lewis acidic nature.

An initial attempt to synthesize the hydride species was conducted by adding $\text{KB}^s\text{Bu}_3\text{H}$ (1 equiv.) to the THF solution of the compound $\{\text{LPb}\}_n$ at $-35\text{ }^\circ\text{C}$. A rapid color change from orange-red to bright yellow was observed immediately upon the addition of $\text{KB}^s\text{Bu}_3\text{H}$. The ^1H NMR spectrum of the reaction mixture, which was obtained within 5 min, revealed formation of a new species ($\text{K}[\text{1-H}]$); a broad resonance was found at $\delta = 39.64$ ppm (full width at half maximum $H = 60$ Hz, see Supplementary Fig. S4). This species however decayed very quickly at room temperature (within 30 min) to produce a black insoluble powder, which was presumably lead metal, together with potassium salt K_2L (potassium salt of dianionic L^{2-}) and H_2 as evidenced by ^1H NMR spectroscopy. The extremely downfield-shifted ^1H resonance is likely attributed to the hydride ligand at the Pb center. The ^1H NMR spectra of the terphenyl-stabilized lead(II) hydrides reported by Wesemann¹² and Power¹³ featured hydride signals located at approximately 33 to 35 ppm. The unusually high frequency of the ^1H NMR shifts of the lead(II) hydrides was predicted theoretically by Vicha and Straka¹⁹, who described the spectroscopic abnormality of a lead(II) hydride species originating from the spin-orbit heavy atom on the light atom effect (i.e., SO-HALA effect)²⁰⁻²³. The ^1H resonance of $\text{K}[\text{1-H}]$ is close to theoretical predictions with respect to monomeric lead hydrides supported by tridentate pincer-type (33.8 ppm) and β -diketiminato (52.5 ppm) ligands¹⁹.

The formation of K_2L as the decomposition product of $\text{K}[\text{1-H}]$ implies that a potassium ion may have been initially substituted for the “PbH” moiety of the $[\text{LPbH}]^-$ ($[\text{1-H}]^-$) anion of $\text{K}[\text{1-H}]$, leading to a sequence of decomposition reactions. The interference of the potassium ion may be excluded by the use of crown ethers, which have high binding affinity toward alkali metal ions. The addition of $\text{KB}^s\text{Bu}_3\text{H}$ to $\{\text{LPb}\}_n$ in the presence of an excess amount of 18-crown-6 (3–4 equiv.) in THF rapidly produced a bright yellow solution, and no decomposition products was observed visually or by ^1H NMR spectroscopy after 3 hours of reaction (Fig. 3). The reaction mixture was subjected to a workup, resulting in the production of $[\text{K18c6}][\text{1-H}]$, a yellow powder, in 81% yield. Although $[\text{K18c6}][\text{1-H}]$ was also soluble in benzene, it decomposed within 3 h. The ^1H NMR spectrum of $[\text{K18c6}][\text{1-H}]$ in d_8 -THF exhibited sharp resonance at $\delta = 41.43$ ppm that was flanked by satellites resulting from $^{207}\text{Pb}-^1\text{H}$ coupling ($^1J_{\text{PbH}} = 1312$ Hz; Fig. 4a). To the best of our knowledge, this unusual ^1H resonance is at the lowest field observed thus far for a diamagnetic compound. The coupling constant of $[\text{K18c6}][\text{1-H}]$ was considerably higher than those reported for $[\text{ArPb}(\mu\text{-H})]_2$ (700–750 Hz)^{12,13}, and it was much lower than that reported for Me_3PbH (2379 Hz)²⁴. The magnitude of the spin–spin coupling constant (J) is directly related to the Fermi contact mechanism²⁴⁻²⁶, and the $^1J_{\text{PbH}}$ of the Pb–H bond is proportional to the percentage of 6s orbitals of Pb involved in this type of bonding. Thus, the coupling constants of low-valent lead(II) hydrides found in $[\text{K18c6}][\text{1-H}]$ and $[\text{Ar}^{\text{IPr}}\text{Pb}(\mu\text{-H})]_2$ were expected to be lower than that of tetravalent Me_3PbH due to the pronounced inert-pair effect in Pb(II) species⁴. The high stability of $[\text{K18c6}][\text{1-H}]$ allowed us to probe the ^{207}Pb NMR resonance of this species. The $^{207}\text{Pb}\{^1\text{H}\}$ NMR spectrum of $[\text{K18c6}][\text{1-H}]$ contains a single sharp resonance at 1450.1 ppm (Fig. 4b). To prove that this resonance is associated with the Pb center in $[\text{K18c6}][\text{1-H}]$, a proton-coupled ^{207}Pb NMR spectrum was obtained, and it exhibits a doublet signal

centered at 1450.1 ppm with a $^1J_{\text{HPb}}$ of 1320 Hz; this finding was consistent with the coupling constant observed in the ^1H NMR spectrum (Fig. 4c). On the basis of ^1H - ^{207}Pb heteronuclear-multiple-quantum-coherence (HMQC) NMR experiments, we were able to observe the correlation between the hydride signal and Pb resonance (Fig. 4d). Furthermore, the ^2H NMR spectrum of the deuterium-labeled species (**[K18c6][1-D]**, *vide infra*) exhibited resonance at 41 ppm (Supplementary Fig. S19), and the species' Pb signal in the $^{207}\text{Pb}\{^1\text{H}\}$ NMR spectrum was broad ($H = 690$ Hz; Fig. 4e) due to deuteride coupling (nuclear spin $I = 1$). $^1J_{\text{PbD}}$ (~ 200 Hz) is expected to be approximately 1/6.5 as large as $^1J_{\text{PbH}}$ because the coupling constants of varying isotopes are proportional to their gyromagnetic ratios ($\gamma_{\text{D}}/\gamma_{\text{H}} = 1/6.488$). The ^{207}Pb NMR resonance of **[K18c6][1-H]** is shifted upfield compared with that of $[\text{Ar}^{\text{iPr}}\text{Pb}(\mu\text{-H})]_2$ (3736 ppm)¹², and it is closer to that of the base-stabilized $[\text{Ar}^{\text{iPr}}\text{PbH}(\text{NHC})]$ (NHC = 1,3,4,5-tetramethylimidazol-2-ylidene; $\delta = 834$ ppm), which possesses higher coordination at the Pb center¹².

Furthermore, the presence of the **[1-H]⁻** moiety of **[K18c6][1-H]** in the THF solution was probed by performing electrospray ionization–mass spectrometry in negative ion-mode, which revealed the presence of **[1-H]⁻** from **[K18c6][1-H]** ($m/z = 720.33$, Supplementary Fig. S23) and **[1-D]⁻** from **[K18c6][1-D]** ($m/z = 721.42$, Supplementary Fig. S24). Finally, infrared spectroscopy was performed to detect Pb–H and Pb–D vibrations. Although no clear Pb–H stretching frequency was identified, likely due to the overlap with other signals, a Pb–D vibration was identified at 1053 cm^{-1} , which was close to the theoretically predicted value 1065 cm^{-1} (Supplementary Fig. S21). Collectively, these spectroscopic findings enabled the unambiguous assignment of the hydride ligand bound to the lead center in **[K18c6][1-H]**.

The half-life ($t_{1/2}$) of **[K18c6][1-H]** is approximately 2 days in THF at ambient temperature, as indicated by the disappearing hydride signal in the ^1H NMR spectrum (Supplementary Fig. S12, *vide infra*). It is also noteworthy when only the equimolar of 18-crown-6 was employed in this reaction, the resulting lead hydride species decomposed within 2 h. This observation indicates that the necessary sequester of K^+ was the key to stabilizing the **[1-H]⁻** moiety. When 1 equiv. of [2.2.2]-cryptand was employed instead of 18-crown-6 as the chelator for the potassium ion, a lead hydride species **[(2.2.2)-cryptand)K][LPbH]** (**[Kcrypt222][1-H]**) was isolated as a yellow powder in 90% yield (Fig. 3). Notably, the compound **[Kcrypt222][1-H]** is much more stable in solution and solid-state form than the compounds **K[1-H]** and **[K18c6][1-H]**. The solid form of **[Kcrypt222][1-H]** can be stored at room temperature and exhibited no observable decomposition for 30 days. Single crystals of **[Kcrypt222][1-H]** were obtained by performing pentane diffusion in the saturated THF solution at $-35\text{ }^\circ\text{C}$, and X-ray crystallography clearly indicated that **[Kcrypt222][1-H]** as an anionic and monomeric plumbylene complex with **[(2.2.2)-cryptand)K]** as the counter ion (Fig. 5a). The lead center is 0.215 \AA out of the ligand plane (defined by three nitrogen atoms), and this deviation is larger than that observed in **10THF₂** (0.024 \AA). Whereas complex **10THF₂** possesses two THF molecules bound to the axial positions, only one ligand (i.e., H^- ligand) is likely bound to the Pb

center and responsible for the displacement of Pb. The crystal packing diagram of **[Kcrypt222][1-H]** exhibits no close contact between the lead centers on separate molecules, indicating that **[Kcrypt222][1-H]** is a distinct, monomeric molecule in the solid-state structure (Supplementary Fig. S26b). The NMR features of **[Kcrypt222][1-H]** and **[K18c6][1-H]** are essentially identical (for the **[1-H]⁻** moiety, Supplementary Fig. S15), and the discussion of the spectroscopic characterization of the **[1-H]⁻** moiety focuses mainly on **[K18c6][1-H]** due to the limited solubility of **[Kcrypt222][1-H]** in THF. The employment of crown ethers to sequester K⁺ appeared to be a valid strategy for enhancing the stability of the **[1-H]⁻** anion. This inference was confirmed by adding KPF₆ as a free K⁺ source to THF solutions containing **[K18c6][1-H]** and **[Kcrypt222][1-H]**, which resulted in the immediate decomposition of the lead hydride species in both cases.

Several factors likely contributed to the uncommon stability of the **[1-H]⁻** moiety, which was observed despite a lack of commonly used sterically demanding substituents (such as the 2,6-diisopropylphenyl and 2,4,6-trimethylphenyl groups in the ligand system) that provide sufficient steric protection. First, dihydrogen bonding (DHB) interactions between the ortho hydrogens on the five-phenyl rings of the pyrrolyl donors (H_{P_h}) and hydride ligand (H_{P_b}) may have stabilized the Pb–H moiety (Fig. 6a). The ¹H one-dimensional nuclear-Overhauser-effect spectroscopy (i.e., 1-D NOSEY) of **[K18c6][1-H]** in d₈-THF at –20 °C revealed a correlation between H_{P_b} and H_{P_h}, suggesting they were in close proximity (Fig. 6b). In the density-functional-theory-optimized structure, two H_{P_h} were pointing toward H_{P_b} at a short distance of 2.317 Å, which was less than the sum of the van der Waals radii of H (2r_H = 2.4 Å; Fig. 4a)²⁷. Our natural bond orbital analysis results further supported the presence of DHB in this system. In particular, natural population analysis revealed that the charges in the hydride (–0.333) and ortho hydrogens (0.233) were consistent with our hypothesis for H_{P_b}^{δ-} × × × H_{P_h}^{δ+} interactions. The results of second-order-perturbation-energy analysis supported our assumption, indicating a donor–acceptor interaction of 1.76 kcal/mol from the Pb–H σ bonding pair to the σ* of ortho C–H bonds. Collectively, the experimental observations and computational results indicated the presence of DHB, which provided secondary coordination sphere interactions in the **[1-H]⁻** moiety and, consequently, stabilized Pb–H bonding. Second, strong donation from the dianionic pincer ligand **L** to the Pb center may have prevented homolytic cleavage of the Pb–H bond, which could have, in turn, led to an anionic [LPb×]⁻ fragment and H× generating dianionic diplumbynes and H₂. Furthermore, the kinetic stabilization provided by the phenyl groups on the pyrrolyl donor should not be neglected in the **[1-H]⁻** moiety.

Low-valent Ge and Sn hydride species readily undergo hydroelementation reactions with carbonyl compounds²⁸⁻³². We discovered that the hydroplumbylation reaction of **[1-H]⁻** with benzaldehyde cleanly produced a Pb(II) benzyloxy compound **[1-OBz]⁻** in 92% yield (for M = [Kcrypt222]). Alternatively, this species could be obtained as orange-yellow crystals in 85% yield by adding Lewis basic potassium benzyloxide to **{LPb}_n** in the presence of [2.2.2]-cryptand (Fig. 3). After hydride transfer to benzaldehyde,

the characteristic downfield lead hydride signal in the ^1H NMR spectrum was replaced by the CH_2 resonance of the benzyloxy group at 5.37 ppm. The ^{207}Pb NMR resonance of **[Kcrypt222][1-OBz]** was identified at $\delta = 847.3$ ppm, indicating an upfield shift relative to **[Kcrypt222][1-H]** (1450.1 ppm). The molecular structure of **[Kcrypt222][1-OBz]**, which was clarified using X-ray crystallography, revealed that the benzyloxy group was bound to the lead center with a Pb–O bond length of 2.153(4) Å (average of two independent molecules in the unit cell) and $\text{N}_{\text{py}}\text{–Pb–O}$ angle (avg.) of 90.16(13)° (Fig. 5b). Interestingly, ortho hydrogens on the five-phenyl rings of the pyrrolyl donors (H_{Ph}) were pointing toward the oxygen atom with averaged $\text{H}_{\text{Ph}}^{\delta+} \times \times \text{O}^{\delta-}$ distances of 2.70 Å. These short distances between partially positive H_{Ph} and partially negative O were reminiscent of the aforementioned DHB interactions. Notably, **[Kcrypt222][1-OBz]** reacted cleanly with HBpin to regenerate the lead hydride species **[Kcrypt222][1-H]** and the borated product BzOBPin; this was verified through ^1H NMR spectroscopy and mass spectrometry. The deuterium-labeled **[1-D]**[−] species was obtained similarly by using DBpin and was obtained in 94% yield. Remarkably, the successful generation of **[1-H]**[−] suggests the use of lead(II) hydride to perform the catalytic hydroboration of carbonyl compounds³.

Discussion

In summary, we report the synthesis of lead(II) hydride complexes with remarkable thermostability, which were achieved with the support of the dianionic pincer ligand **L**. Multiple spectroscopic tools (such as $^{207}\text{Pb}\{^1\text{H}\}$, proton-coupled ^{207}Pb , and $^1\text{H}\text{-}^{207}\text{Pb}$ HMQC NMR spectroscopy, and mass spectrometry of **[1-H]**[−] and **[1-D]**[−] anions) enabled unambiguous assignment of lead-hydride (or deuteride) bonds. In addition to the strong donating nature of **L**, the roles of DHB (secondary coordination sphere interaction) and the steric bulkiness of **L** were essential in stabilizing the monomeric and anionic lead hydride complexes, as demonstrated by the experimental and computational results. Finally, the regeneration of lead(II) hydrides from benzyloxy compound through the use of HBpin indicated that lead(II) hydride can be used as a catalyst for carbonyl hydroboration reactions.

Methods

General considerations

All manipulations with oxygen and moisture sensitive materials were performed in a nitrogen-filled glovebox. Solvents were dried and deaerated using a solvent system (AsiaWong Enterprise co., Ltd.) prior to use. Benzene- d_6 and tetrahydrofuran- d_8 (THF- d_8) was dried over sodium and benzophenone, degassed by three freeze-pump-thaw cycles, and stored under nitrogen over 3 Å molecular sieves. $\text{KB}^s\text{Bu}_3\text{H}$ (K-selectride) was purchased from Sigma-Aldrich, used as received and stored in freezer of a glovebox. [2.2.2]-cryptand (4,7,13,16,21,24-Hexaoxa-1,10-diazabicyclo[8.8.8]hexacosane) and 18-crown-6 (1,4,7,10,13,16-Hexaoxacyclooctadecane) were purchased from Sigma-Aldrich, used as received and

stored in a glovebox. The compounds H_2L ,¹⁵ $\text{Pb}(\text{HMDS})_2$ ³³ and DBpin ³⁴ were prepared according to literature procedures.

Synthesis of LPbTHF_2 (1-THF₂). A solution of $\text{Pb}(\text{HMDS})_2$ (719.5 mg, 1.36 mmol) in 5 mL of toluene was added to a solution of H_2L (699.9 mg, 1.36 mmol) in 10 mL of toluene at ambient temperature. The solution turned to red from yellow immediately and resulted in visible precipitates. After stirring at ambient temperature for 13 h, the mixture was cooled to -35°C , and the supernatant was removed by decanting. The remaining solid was washed three times with 10 mL of pentane and then dried under vacuum to afford a red-orange powder $\{\text{LPb}\}_n$. Yield: 930.5 mg (95%). This product is barely soluble in benzene or toluene, whereas it reacts with THF to form the monomeric adduct **1-THF₂** that is soluble in THF. Red-orange crystals were obtained by diffusion of pentane into the saturated THF solution at -35°C for 5 days. Yield: 85%.

Synthesis of [K18c6][1-H]. A solution of k-selectride (48.6 μL , 0.049 mmol) in 1.5 mL THF was cooled at -35°C and was added dropwise to a precooled solution containing $\{\text{LPb}\}_n$ (35.2 mg, 0.049 mmol) and excess 18-crown-6 (32.1 mg, 0.121 mmol) in 5 mL THF. The clear orange red solution turned yellow was observed upon addition. The mixture was warmed to ambient temperature and stirred for 10 minutes, and was concentrated under vacuum to ca. 2 mL. Addition of pentane resulted in the formation of a yellow powder, and the supernatant was removed by decanting. The remaining solid was washed three times with 5 mL of pentane and then dried under vacuum to afford a yellow powder.

Synthesis of [Kcrypt222][1-H]. A solution of k-selectride (208.9 μL , 0.209 mmol) in 1.5 mL THF was cooled at -35°C and was added dropwise to a precooled solution containing $\{\text{LPb}\}_n$ (150.2 mg, 0.209 mmol) and [2.2.2]-cryptand (78.6 mg, 0.209 mmol) in 10 mL THF. The clear orange red solution turned yellow was observed upon addition. The mixture was warmed to ambient temperature and stirred for 10 minutes, and the volume of the solution was concentrated under vacuum to ca. 2 mL. Diffusion of pentane into the filtered and saturated THF solution at -35°C afforded yellow crystals of [Kcrypt222][1-H]. Yield: 213.5 mg (90%).

Synthesis of [Kcrypt222][1-OBz].

Method 1: Benzaldehyde (3.8 mg, 0.036 mmol) was added to a precooled solution of [Kcrypt222][1-H] (40.6 mg, 0.036 mmol) in 10 mL THF at -35°C , and the resulting solution was stirred at ambient temperature for 1 hr. The cloudy yellow solution turned into a clear orange-yellow solution was observed immediately. The solution was filtered through a plug of Celite, and the filtrate was dried under vacuum. Yield: 40.22 mg (90%). Cooling down the hot, saturated benzene solution of [Kcrypt222][1-OBz] afforded analytically pure yellow crystals.

Method 2: A precooled solution of potassium benzyloxide (4.12 mg, 0.028 mmol) in 2 mL THF was added to a THF solution containing $\{\text{LPb}\}_n$ (20.3 mg, 0.028 mmol), and [2.2.2]-cryptand (10.8 mg, 0.029 mmol) at -35°C . The resulting solution turned orange yellow was observed and stirred at room temperature for 2

hrs. The solution was filtered through a plug of Celite, and the filtrate was dried under vacuum. Yield: 29.8 mg (85%).

[K18c6][1-OBz] can be obtained in a similar procedure with yield of 26.1 mg (82%).

Synthesis of [K18c6][1-D]. To a precooled solution of **[K18c6][1-OBz]** (19.8 mg, 0.017 mmol) in THF, deuterated pinacolborane (DBpin, 0.138 M in C₆D₆, 127 μL, 0.017 mmol) was added, and the mixture was stirred at room temperature for 10 mins. The solution was then concentrated under vacuum to ca. 2 mL. Addition of pentane resulted in the formation of a yellow powder, and the supernatant was removed by decanting. The remaining solid was washed three times with 5 mL of pentane and then dried under vacuum to afford a yellow powder **[K18c6][1-D]**. Yield: 45.5 mg (81%). **[Kcrypt222][1-D]** can be obtained in a similar manner with yield of 36.8 mg (94%).

Theoretical methods

Density Functional Theory (DFT) calculations were performed with the Gaussian 16 suite of programs.³⁵ Geometry optimizations were applied by the means of the PBE0³⁶ hybrid functional, corrected for dispersion as proposed by Grimme (D3 correction, BJ damping),^{37,38} and performed without any symmetry constraints using 6-311G(d,p) basis set for H, C, and N, and Def2-TZVP³⁹ basis set for Pb. NBO analyses were performed with NBO 6.0.⁴⁰ Input structures were taken from the experimentally observed X-ray diffraction structures of the anion **[1-H]** part of **[Kcrypt222][1-H]**.

Single-crystal X-ray diffraction

Single-crystal X-ray diffraction were performed on a Bruker APEX DUO diffractometer with APEX II 4K and multi-layer mirror monochromated Mo K_α radiation ($\lambda = 0.71073 \text{ \AA}$) at 200(2) K. Data collection and reduction were performed with Bruker APEX II software. All of non-hydrogen atoms are refined anisotropically. Hydrogen atoms attached to the carbons were fixed at calculated positions and refined using a riding mode. Multiple disordered solvent molecules were observed in the crystal structures of all complexes. Whenever possible, co-crystallizing solvent molecules were modeled. Otherwise, SQUEEZE was employed to treat diffuse solvent contribution in the voids.

Data Availability

CCDC 2068336 **LPb(THF)**₂ (1), CCDC 2102361 **[Kcrypt222][1-H]**, and CCDC 2102361 **[Kcrypt222][1-OBz]** contain the supplementary crystallographic data for this paper. These data can be obtained free of charge from The Cambridge Crystallographic Data Centre via www.ccdc.cam.ac.uk/data_request/cif.

Declarations

Acknowledgements (optional)

This work was funded by Taiwan's Ministry of Science and Technology (MOST) under grant no. 108-2636-M-009-006, 109-2636-M-009-004, and 110-2636-M-009-003 (Young Scholar Fellowship Program). S.W. and H.-J.Liu thank Prof. Hsin-Tien Chiu for helpful discussions.

Ethics declarations

The authors declare no competing financial interest.

Supplementary Information

General considerations, synthetic procedures, NMR spectra, theoretical calculation details, and crystallographic data for all compounds are included in the Supporting Information.

References

1. Eichler, B. E. & Power, P. P. [2,6-Trip₂H₃C₆Sn(μ-H)]₂ (Trip = C₆H₂-2,4,6-i-Pr₃): Synthesis and Structure of a Divalent Group 14 Element Hydride. *J. Am. Chem. Soc.* **122**, 8785–8786, (2000).
2. Mandal, S. K. & Roesky, H. W. Group 14 Hydrides with Low Valent Elements for Activation of Small Molecules. *Acc. Chem. Res.* **45**, 298–307, (2012).
3. Hadlington, T. J., Driess, M. & Jones, C. Low-valent group 14 element hydride chemistry: towards catalysis. *Chem. Soc. Rev.* **47**, 4176–4197, (2018).
4. Pyykko, P. Relativistic effects in structural chemistry. *Chem. Rev.* **88**, 563–594, (1988).
5. Neumann, W. P. & Kühlein, K. Hydroplumbation of Unsaturated Organic Compounds. *Angew. Chem. Int. Ed. Engl.* **4**, 784–785, (1965).
6. Juenge, E. C., Hawkes, S. J. & Snider, T. E. Preparation of butadienyl- and butenyl-plumbanes and -stannanes, by hydroplumbylation and hydrostannylation of vinylacetylene and 1-butyne including in situ techniques. *J. Organomet. Chem.* **51**, 189–195, (1973).
7. Wang, X. & Andrews, L. Infrared Spectra of Group 14 Hydrides in Solid Hydrogen: Experimental Observation of PbH₄, Pb₂H₂, and Pb₂H₄. *J. Am. Chem. Soc.* **125**, 6581–6587, (2003).
8. Cho, H.-G. & Andrews, L. Infrared Spectra of CH₃-MH through Methane Activation by Laser-Ablated Sn, Pb, Sb, and Bi Atoms. *J. Phys. Chem. A* **116**, 8500–8506, (2012).
9. Xu, B. *et al.* Matrix-Infrared Spectra and Structures of HM-SiH₃ (M = Ge, Sn, Pb, Sb, Bi, Te Atoms). *J. Phys. Chem. A* **122**, 81–88, (2018).
10. Villegas-Escobar, N. *et al.* Why Low Valent Lead(II) Hydride Complex Would be a Better Catalyst for CO₂ Activation than Its 14 Group Analogues? *J. Phys. Chem. C* **121**, 12127–12135, (2017).
11. Schneider, J., Sindlinger, C. P., Freitag, S. M., Schubert, H. & Wesemann, L. Diverse Activation Modes in the Hydroboration of Aldehydes and Ketones with Germanium, Tin, and Lead Lewis Pairs. *Angew. Chem. Int. Ed.* **56**, 333–337, (2017).

12. Schneider, J., Sindlinger, C. P., Eichele, K., Schubert, H. & Wesemann, L. Low-Valent Lead Hydride and Its Extreme Low-Field ^1H NMR Chemical Shift. *J. Am. Chem. Soc.* **139**, 6542–6545, (2017).
13. Queen, J. D., Fetting, J. C. & Power, P. P. Two quasi-stable lead(ii) hydrides at ambient temperature. *Chem. Commun.* **55**, 10285–10287, (2019).
14. Chang, W.-C. *et al.* Linear, mixed-valent homocatenated tri-tin complexes featuring Sn–Sn bonds. *Chem. Commun.* **56**, 6786–6789, (2020).
15. Nagata, T. & Tanaka, K. Syntheses of a 6-(2-Pyrrolyl)-2,2'-bipyridine Derivative and Its Ruthenium Complex. *Bull. Chem. Soc. Jpn.* **75**, 2469–2470, (2002).
16. Hitchcock, P. B., Lappert, M. F. & Protchenko, A. V. New reactions of β -diketiminatolanthanoid complexes: sterically induced self-deprotonation of β -diketiminato ligands. *Chem. Commun.*, 951–953, (2005).
17. Yao, S., Block, S., Brym, M. & Driess, M. A new type of heteroleptic complex of divalent lead and synthesis of the P-plumbyleniophosphasilene, $\text{R}_2\text{Si}=\text{P}-\text{Pb}(\text{L})$: (L = β -diketimate). *Chem. Commun.*, 3844–3846, (2007).
18. Jana, A. *et al.* Facile Access of Well-Defined Stable Divalent Lead Compounds with Small Organic Substituents. *Organometallics* **28**, 2563–2567, (2009).
19. Vícha, J., Marek, R. & Straka, M. High-Frequency ^1H NMR Chemical Shifts of SnII and PbII Hydrides Induced by Relativistic Effects: Quest for PbII Hydrides. *Inorg. Chem.* **55**, 10302–10309, (2016).
20. Pyykkö, P., Görling, A. & Rösch, N. A transparent interpretation of the relativistic contribution to the N.M.R. 'heavy atom chemical shift'. *Mol. Phys.* **61**, 195–205, (1987).
21. Kaupp, M., Malkina, O. L., Malkin, V. G. & Pyykkö, P. How Do Spin–Orbit-Induced Heavy-Atom Effects on NMR Chemical Shifts Function? Validation of a Simple Analogy to Spin–Spin Coupling by Density Functional Theory (DFT) Calculations on Some Iodo Compounds. *Chem. Eur. J.* **4**, 118–126, (1998).
22. Vícha, J., Straka, M., Munzarová, M. L. & Marek, R. Mechanism of Spin–Orbit Effects on the Ligand NMR Chemical Shift in Transition-Metal Complexes: Linking NMR to EPR. *J. Chem. Theory Comput.* **10**, 1489–1499, (2014).
23. Vícha, J., Marek, R. & Straka, M. High-Frequency ^{13}C and ^{29}Si NMR Chemical Shifts in Diamagnetic Low-Valence Compounds of TII and PbII: Decisive Role of Relativistic Effects. *Inorg. Chem.* **55**, 1770–1781, (2016).
24. Flitcroft, N. & Kaesz, H. D. Proton Magnetic Resonance in Stannane, the Methylstannanes and Related Compounds. *J. Am. Chem. Soc.* **85**, 1377–1380, (1963).
25. Ramsey, N. F. Electron Coupled Interactions between Nuclear Spins in Molecules. *Phys. Rev.* **91**, 303–307, (1953).
26. Karplus, M. & Anderson, D. H. Valence-Bond Interpretation of Electron-Coupled Nuclear Spin Interactions; Application to Methane. *J. Chem. Phys.* **30**, 6–10, (1959).
27. Bondi, A. van der Waals Volumes and Radii. *J. Phys. Chem.* **68**, 441–451, (1964).

28. Jana, A., Roesky, H. W. & Schulzke, C. Reactivity of germanium(II) hydride with nitrous oxide, trimethylsilyl azide, ketones, and alkynes and the reaction of a methyl analogue with trimethylsilyl diazomethane. *Dalton Trans.* **39**, 132–138, (2010).
29. Jana, A. *et al.* A Germanium(II) Hydride as an Effective Reagent for Hydrogermylation Reactions. *J. Am. Chem. Soc.* **131**, 1288–1293, (2009).
30. Jana, A., Roesky, H. W., Schulzke, C. & Döring, A. Reactions of Tin(II) Hydride Species with Unsaturated Molecules. *Angew. Chem. Int. Ed.* **48**, 1106–1109, (2009).
31. Hadlington, T. J., Hermann, M., Frenking, G. & Jones, C. Low Coordinate Germanium(II) and Tin(II) Hydride Complexes: Efficient Catalysts for the Hydroboration of Carbonyl Compounds. *J. Am. Chem. Soc.* **136**, 3028–3031, (2014).
32. Hadlington, T. J., Kefalidis, C. E., Maron, L. & Jones, C. Efficient Reduction of Carbon Dioxide to Methanol Equivalents Catalyzed by Two-Coordinate Amido–Germanium(II) and – Tin(II) Hydride Complexes. *ACS Catal.* **7**, 1853–1859, (2017).
33. Glock, C. *et al.* Calcium, Strontium, Germanium, Tin, and Lead bis(trimethylsilyl)amido Derivatives and 2,2,6,6-Tetramethylpiperidido and N-isopropylphenylamido Derivatives of Potassium and Calcium. *Inorg. Synth.*, 15–31, (2018).
34. Espinal-Viguri, M., Neale, S. E., Coles, N. T., Macgregor, S. A. & Webster, R. L. Room Temperature Iron-Catalyzed Transfer Hydrogenation and Regioselective Deuteration of Carbon–Carbon Double Bonds. *J. Am. Chem. Soc.* **141**, 572–582, (2019).
35. Gaussian 16 Rev. C.01 (Wallingford, CT, 2016).
36. Adamo, C. & Barone, V. Toward reliable density functional methods without adjustable parameters: The PBE0 model. *J. Chem. Phys.* **110**, 6158–6170, (1999).
37. Grimme, S., Antony, J., Ehrlich, S. & Krieg, H. A consistent and accurate ab initio parametrization of density functional dispersion correction (DFT-D) for the 94 elements H–Pu. *J. Chem. Phys.* **132**, 154104, (2010).
38. Grimme, S., Ehrlich, S. & Goerigk, L. Effect of the damping function in dispersion corrected density functional theory. *J. Comput. Chem.* **32**, 1456–1465, (2011).
39. Weigend, F. & Ahlrichs, R. Balanced basis sets of split valence, triple zeta valence and quadruple zeta valence quality for H to Rn: Design and assessment of accuracy. *Phys. Chem. Chem. Phys.* **7**, 3297–3305, (2005).
40. Glendening, E. D., Landis, C. R. & Weinhold, F. NBO 6.0: Natural bond orbital analysis program. *J. Comput. Chem.* **34**, 1429–1437, (2013).

Figures

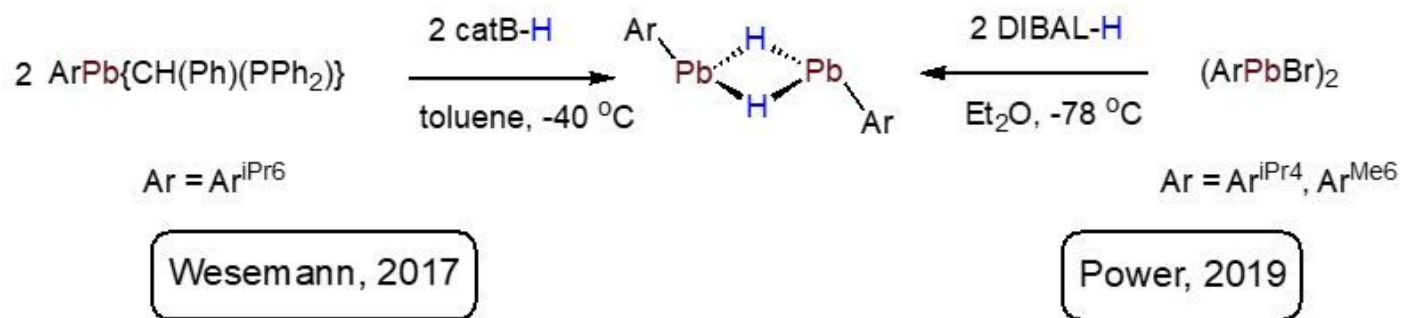


Figure 1

Reaction scheme of the preparation of dimeric Pb(II) hydrides by the Wesemann and Power groups.

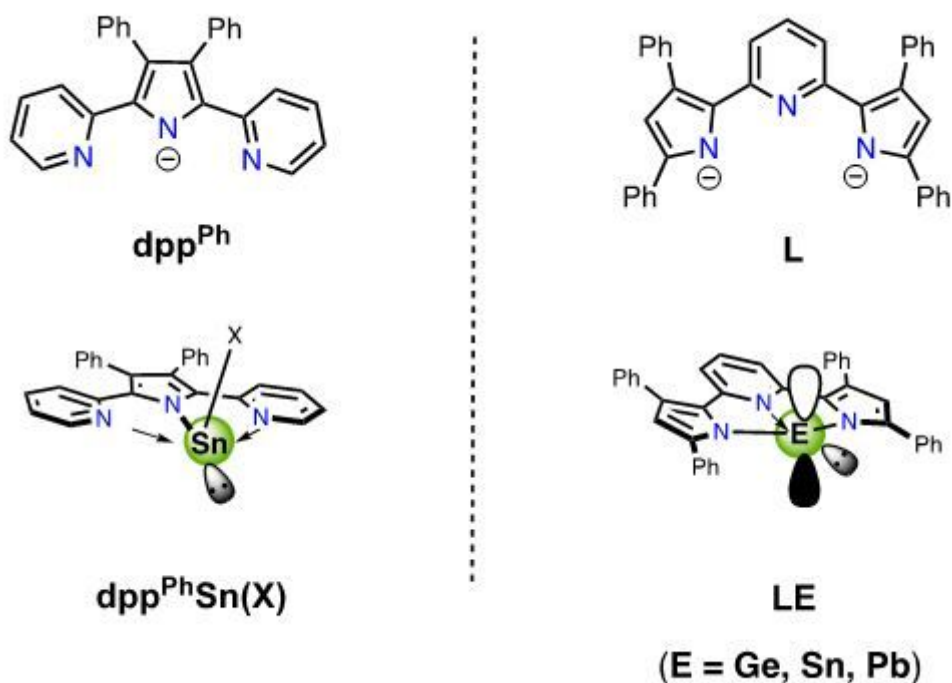
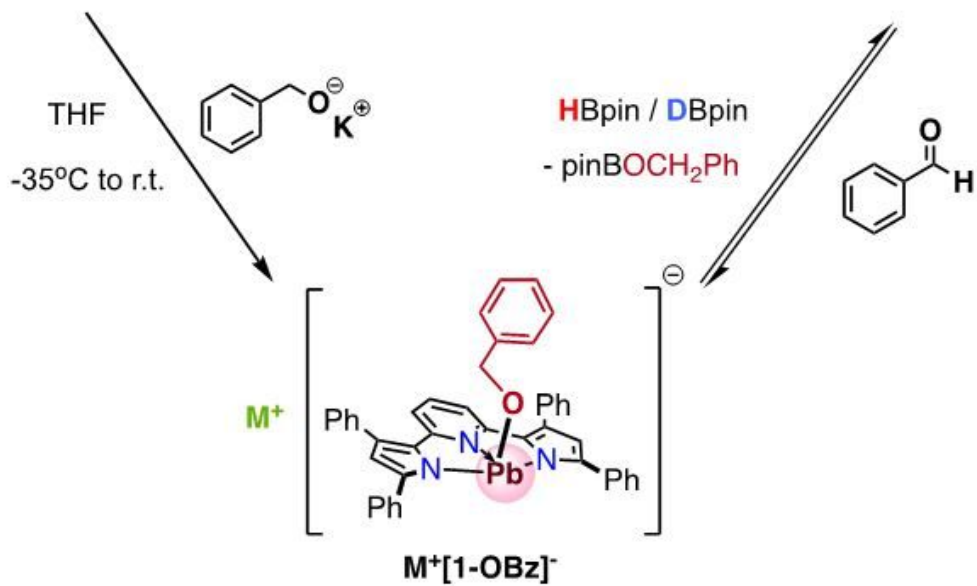
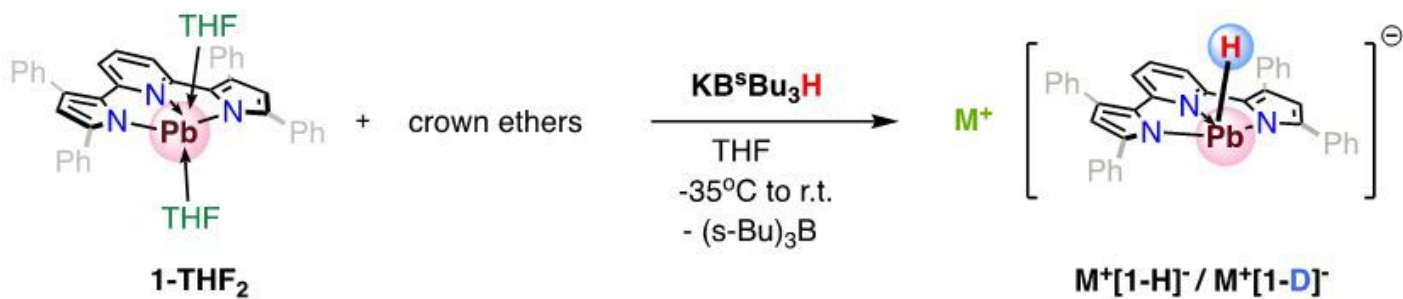


Figure 2

Comparison of the tin(II) center supported by monoanionic dppPh (left) and E(II) (for E = Ge, Sn, and Pb) supported by a dianionic L ligand (right).



$\text{M}^+ = [\text{K18c6}] \text{ ((18-crown-6)potassium)} \text{ or } [\text{Kcrypt222}] \text{ ([2.2.2]-crypt)potassium}$

Figure 3

Reaction scheme of the formation of $\text{M}[\text{1-H}]$ via different synthetic routes.

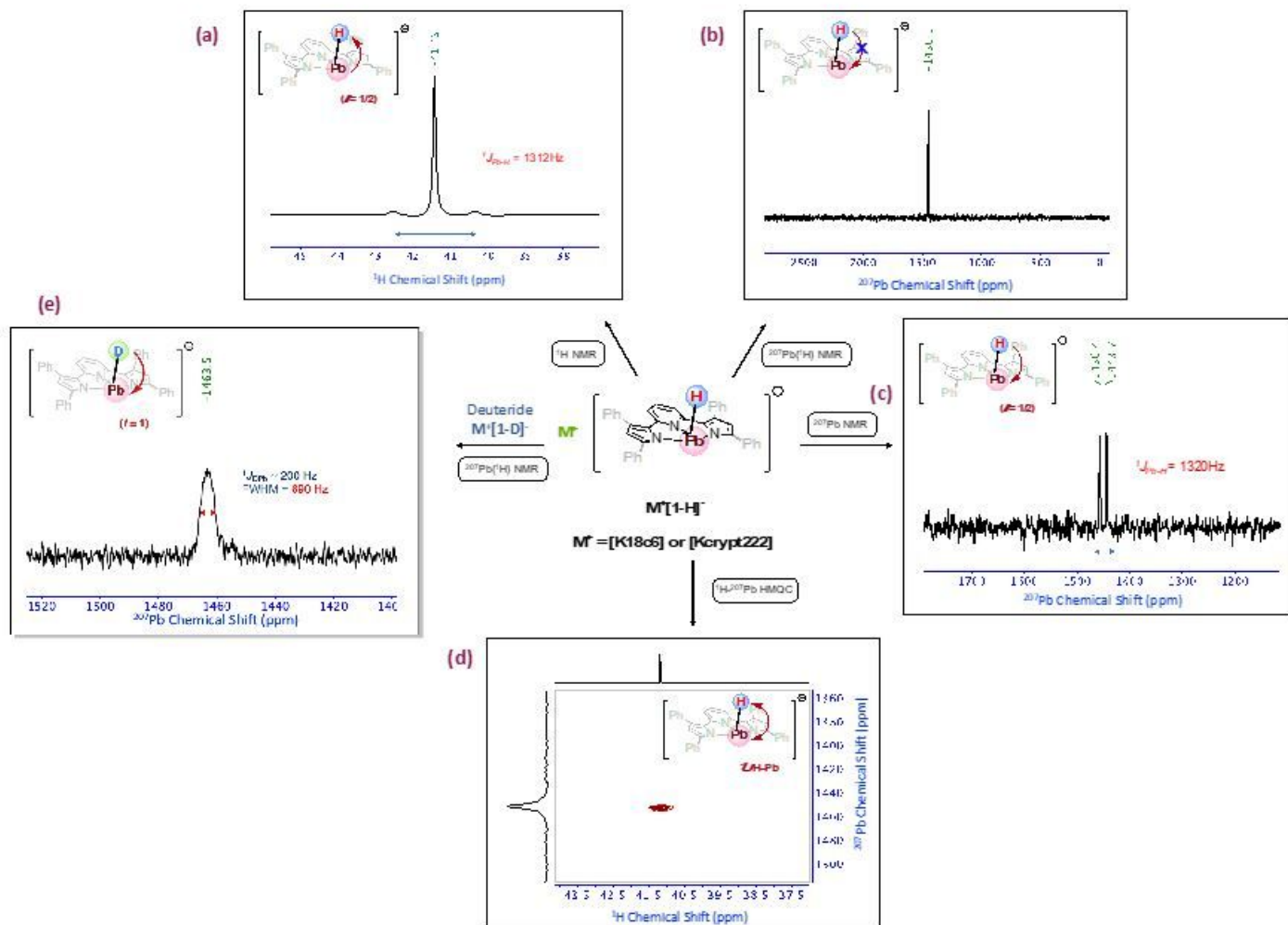


Figure 4

(a) ^1H resonance of hydride ligand of $[\text{K18c6}][1\text{-H}]$; (b) $^{207}\text{Pb}\{^1\text{H}\}$ NMR spectrum of $[\text{K18c6}][1\text{-H}]$; (c) proton-coupled ^{207}Pb NMR spectrum of $[\text{K18c6}][1\text{-H}]$; (d) ^1H - ^{207}Pb HMQC NMR spectrum of $[\text{K18c6}][1\text{-H}]$; and (e) $^{207}\text{Pb}\{^1\text{H}\}$ NMR of $[\text{K18c6}][1\text{-D}]$.

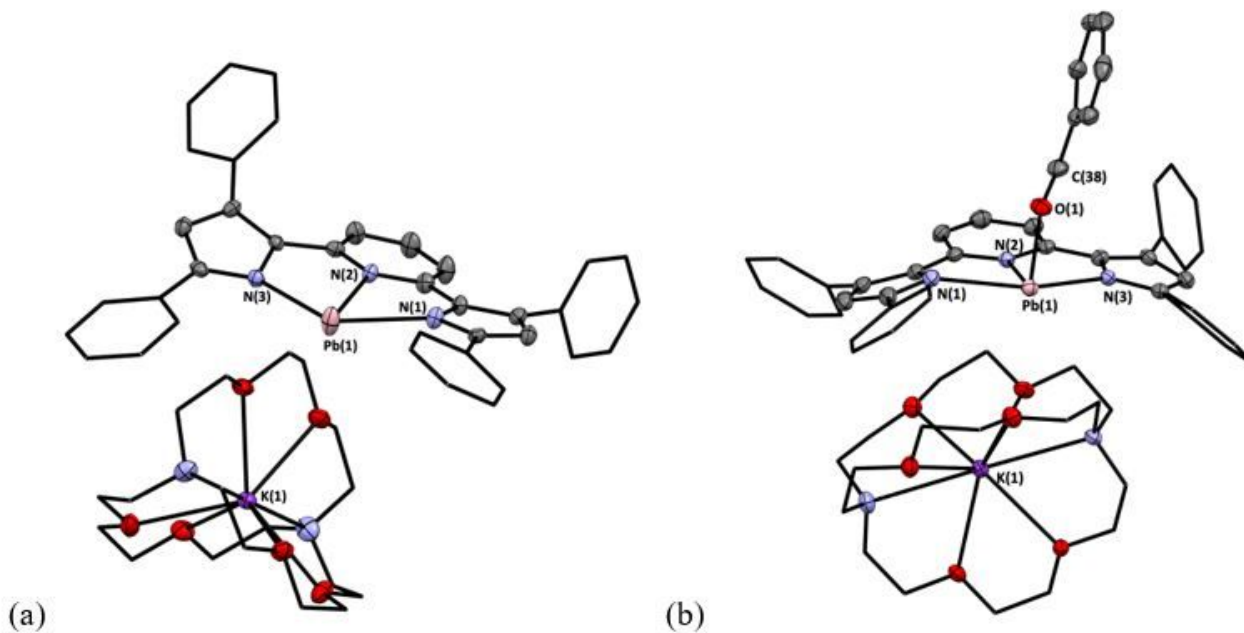


Figure 5

X-ray structures (30% probability ellipsoids) of (a) [Kcrypt222][1-H] and (b) one copy of [Kcrypt222][1-OBz] in an unit cell. H atoms have been omitted for clarity. For (a), one phenyl ring (close to N(1)) was involved in a two-part disorder (total occupancy: 50%), and one of disorder part has been removed for clarity, see Supplementary Fig. S26a.

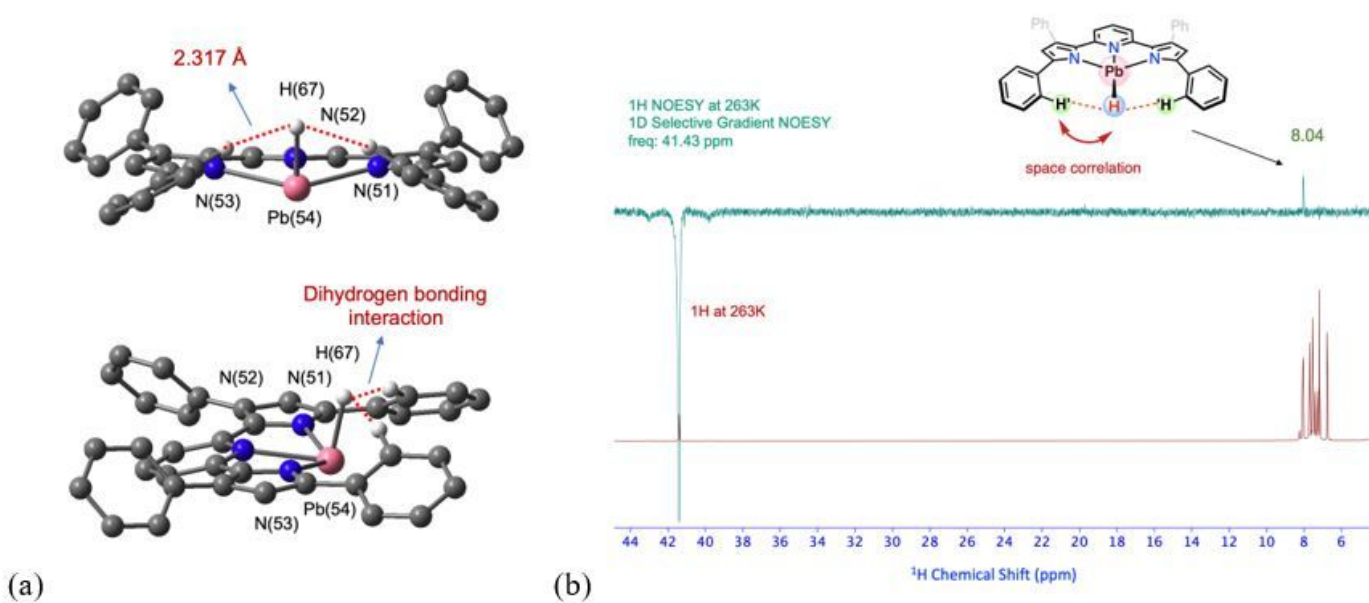


Figure 6

(a) Optimized structure of the [1-H]⁻ moiety indicating a HPb δ^- ...HPh δ^+ distance of 2.317 Å; (b) 1-D NOSEY spectrum (shown in green) on top of ¹H NMR spectrum (in red) of [K18c6][1-H] in d8-THF at -20 °C.

Supplementary Files

This is a list of supplementary files associated with this preprint. Click to download.

- [d22320a.cif](#)
- [d22124.cif](#)
- [d22727.cif](#)
- [SIPbH08122021WSHJ.pdf](#)